Demonstration of an oligosaccharide-diphosphodolichol diphosphatase activity whose subcellular localization is different than those of dolichyl-phosphate-dependent enzymes of the dolichol cycle

Ahmad Massarweh, Michaël Bosco, Soria Iatmanen-Harbi, Clarice Tessier, Nicolas Auberger, Patricia Busca, Isabelle Chantret, Christine Gravier-Pelletier, Stuart Moore

Demonstration of an oligosaccharide-diphosphodolichol diphosphatase activity whose subcellular localization is different than those of dolichyl-phosphate-dependent enzymes of the dolichol cycle

Ahmad Massarweh,*,†,§ Michaël Bosco, Soria Iatmanen-Harbi,*,† Clarice Tessier,*,† Nicolas Auberger,** Patricia Busca,** Isabelle Chantret,*,† Christine Gravier-Pelletier,** and Stuart E. H. Moore[1],*,†**

INSERM U1149,* Paris, France; Université Denis Diderot,† Paris 7, Paris, France; Université Paris Descartes,** CICB-Paris, CNRS UMR8601, LCBPT, Paris, France; and Université Pierre et Marie Curie, Paris 6,§ Paris, France

Abstract Oligosaccharyl phosphates (OSPs) are hydrolyzed from oligosaccharide-diphosphodolichol (DLO) during protein *N*-glycosylation by an uncharacterized process. An OSP-generating activity has been reported in vitro, and here we asked if its biochemical characteristics are compatible with a role in endoplasmic reticulum (ER)-situated DLO regulation. We demonstrate a Co^{2+}-dependent DLO diphosphatase (DLODP) activity that splits DLO into dolichyl phosphate and OSP. DLODP has a pH optimum of 5.5 and is inhibited by vanadate but not by NaF. Polyprenyl diphosphates inhibit [^{3}H]OSP release from [^{3}H]DLO, the length of their alkyl chains correlating positively with inhibition potency. The diphosphodiester $GlcNAc_2$-PP-solanesol is hydrolyzed to yield $GlcNAc_2$-P and inhibits [^{3}H]OSP release from [^{3}H]DLO more effectively than the diphosphomonoester solanesyl diphosphate. During subcellular fractionation of liver homogenates, DLODP codistributes with microsomal markers, and density gradient centrifugation revealed that the distribution of DLODP is closer to that of Golgi apparatus-situated UDP-galactose glycoprotein galactosyltransferase than those of dolichyl-P-dependent glycosyltransferases required for DLO biosynthesis in the ER. Therefore, a DLODP activity showing selectivity toward lipophilic diphosphodiesters such as DLO, and possessing properties distinct from other lipid phosphatases, is identified. Separate subcellular locations for DLODP action and DLO biosynthesis may be required to prevent uncontrolled DLO destruction.—Massarweh, A., M. Bosco, S. Iatmanen-Harbi, C. Tessier, N. Auberger, P. Busca, I. Chantret, C. Gravier-Pelletier, and S. E. H. Moore. **Demonstration of a DLO diphosphatase activity whose subcellular localization is different than those of dolichyl-phosphate-dependent enzymes of the dolichol cycle. *J. Lipid Res.* 2016. 57: 1029–1042.**

Supplementary key words oligosaccharide-diphosphodolichol • endoplasmic reticulum • Golgi apparatus • isoprenoids • phosphatases • phospholipids/trafficking • *N*-linked glycosylation • dolichol-linked oligosaccharide • oligosaccharide-diphosphodolichol diphosphatase • EC 3.6.1.44 • oligosaccharyl phosphates

Protein *N*-glycosylation is essential for embryonic development (1), and children born with deficits in this metabolic pathway often have severe multisystemic diseases called congenital disorders of glycosylation (CDG) (2). *N*-glycosylation begins by transfer of the oligosaccharide, $Glc_3Man_9GlcNAc_2$, from oligosaccharide-diphosphodolichol (DLO; $Glc_3Man_9GlcNAc_2$-PP-dolichol) onto nascent polypeptides in the endoplasmic reticulum (ER) by oligosaccharyltransferase (OST) (3). Dolichyl diphosphate (DolPP), the by-product of OST-mediated protein glycosylation, is recycled to yield dolichyl phosphate (DolP) (4), which is required for the synthesis of GlcNAc-PP-dolichol, dolichyl-P-Man, and dolichyl-P-Glc (5). The former molecule is elongated to yield $Glc_3Man_9GlcNAc_2$-PP-dolichol by UDP-GlcNAc-, GDP-Man-,

Abbreviations: ALP, alkaline phosphatase; CNX, calnexin; Cst, castanospermine; DGPP, diacylglycerol diphosphate; DLO, oligosaccharide-diphosphodolichol; DLODP, DLO diphosphatase; DolP, dolichyl phosphate; DolPP, dolichyl diphosphate; DPMS, dolichyl-P-mannose synthase; DPAGT, UDP-GlcNAc-DolP-GlcNAc 1-P phosphotransferase; DPGS, dolichyl-P-glucose synthase; endo H, endo-β-*N*-acetylglucosaminidase H; ER, endoplasmic reticulum; GA, Golgi apparatus; GlcNAc, *N*-acetylglucosamine; Kif, kifunensin; LPA, lysophosphatidic acid; NCCR, NADPH cytochrome *c* reductase; nfOS, neutral free oligosaccharide; nfOS/S, nfOS plus other neutral sugar; OSP, oligosaccharyl phosphate; OSPP, oligosaccharyl diphosphate; OST, oligosaccharyltransferase; PA, phosphatidic acid; PDI, protein disulphide isomerase; QAE, quaternary aminoethyl; Sw, swainsonine; UGT, UDP-galactose glycoprotein galactosyltransferase.

[1]To whom correspondence should be addressed.
e-mail: stuart.moore@inserm.fr

This work is supported by Fondation pour la Recherche Médicale (FRM Projet: DCM20121225751), the European Union Sixth Framework Programme (LSHM-CT-2005-512131), the E-Rare-2 Joint Transnational Call 2011 (EURO-CDG), and institutional funding from INSERM. A. Massarweh is supported by a joint doctoral fellowship from the French government/An-Najah National University in Palestine.

Manuscript received 24 February 2016 and in revised form 1 April 2016.

Published, JLR Papers in Press, April 1, 2016
DOI 10.1194/jlr.M067330

dolichyl-P-Man- and dolichyl-P-Glc-requiring glycosyltransferases. These ER-situated reactions constitute the dolichol cycle and are controlled at many levels including feedback inhibition (6) and DLO deglucosylation and hydrolysis (7). Neutral free oligosaccharides (nfOSs) can be hydrolyzed from mature DLO by OST (7, 8), and oligosaccharyl phosphates (OSPs) derived from DLO have been shown to occur at low levels in mammalian tissues and cultured cells. OSPs with truncated oligosaccharide structures occur at elevated levels when the corresponding truncated DLOs accumulate in cells with defects in the dolichol cycle, including those from CDG patients, and glucose-starved cells (9–13). Attempts to understand the significance of OSP generation have been hampered because enzymes responsible for this process have not been characterized at the biochemical or molecular levels. Membrane preparations of yeast and mammalian origins have been reported to contain Ca^{2+}- and Mn^{2+}-activated enzymes, respectively, capable of liberating OSP from DLO. Although these activities have been called pyrophosphatases [International Union of Biochemistry and Molecular Biology (IUBMB) nomenclature: oligosaccharide-diphosphodolichol diphosphatase (DLODP), EC 3.6.1.44] (14), a formal demonstration that this type of reaction actually occurs has yet to be presented. In fact, DLO could be split by either a diphosphatase to yield OSP and DolP or a phospholipase-like enzyme to yield dolichol and an oligosaccharyl diphosphate (OSPP) intermediate that could subsequently be rapidly dephosphorylated to yield OSP (15). Finally, whether the biochemical profile of this in vitro activity is compatible with a role in DLO regulation has not been addressed.

In the present report, we describe a membrane-associated, Co^{2+}-activated, DLO-hydrolyzing activity whose pH optimum is 5.5. This activity has a biochemical profile that distinguishes it from other DolP and DolPP phosphatases and hydrolyzes both truncated and mature DLO to yield OSP and DolP, demonstrating for the first time DLODP activity. The selective interaction of DLODP with lipophilic diphosphodiesters indicates that DLOs are potential physiological substrates for this enzyme. Nevertheless, subcellular fractionation studies suggest that DLO biosynthetic reactions and DLODP action are compartmentalized differently.

MATERIALS AND METHODS

Reagents

D-[2-^{3}H(N)]mannose (24.7 Ci/mmol), D-[6-^{3}H(N)]glucosamine (25.9 Ci/mmol), guanosine 5′-diphosphate[1-^{3}H]mannose, [5-^{3}H]mevanolactone (20 Ci/mmol), UDP-[6-^{3}H]*N*-acetylglucosamine (37.0 Ci/mmol), and En^{3}hance spray were from PerkinElmer Life Sciences (Zaventem, Belgium). Dolichyl C_{95}[1-^{3}H]monophosphate (20 Ci/mmol), *RS*-[5-^{3}H]mevalonolactone (50–60 Ci/mmol), and UDP-[1-^{3}H]galactose (15–30 Ci/mmol) were from BIOTREND Chemikalien GmbH (Köln, Germany). UDP-[U-^{14}C]glucose (348 mCi/mmol) was from Amersham International plc. TLC plates were from Merck (Darmstadt, Germany). Dowex resins, fucose, 2-acetamido-2-deoxy-1,3,4,6-tetra-*O*-acetyl-α-D-glucopyranose, endo-β-*N*-acetylglucosaminidase H (endo H) from *Streptomyces plicatus*, protease inhibitor cocktail, protease, Kodak X-Omat film, and alkaline phosphatase (ALP) were purchased from Sigma-Aldrich SARL (St. Quentin Fallavier, France). Castanospermine (Cst), kifunensin (Kif), and swainsonine (Sw) were from Toronto Research Chemicals Inc. (Toronto, Ontario, Canada). The antibodies used are anti-calnexin (CNX) (BD Biosciences, product number 610524) and anti-protein disulphide isomerase (PDI) (Cell Signaling Technology, product number 2446). NuPage LDS sample buffer was from Life Technologies (Cergy Pontoise, France). The Luminol ECL detection system was from Millipore.

Synthesis of DLO analogs

Solanesol- and citronellol-based DLO analog syntheses were performed according to literature procedures (16–23) and will be described in detail in a separate study.

Cell culture

HepG2 cells and the Thy^{-1}, DPM1-deficient, mouse lymphoma cell line (24) were from ATCC (Rockville, MD) and were cultivated at 37°C under an atmosphere containing 5% CO_2 in RPMI 1640 Glutamax™ medium containing 10% FCS and 1% penicillin/streptomycin.

Metabolic radiolabeling of cells

For generation of $Glc_{3\text{-}0}$[^{3}H]$Man_{9\text{-}8}GlcNAc_2$-PP-dolichol, or $Glc_{3\text{-}0}Man_{9\text{-}8}$[^{3}H]$GlcNAc_2$-PP-dolichol, HepG2 cells were rinsed with RPMI 1640 medium containing 0.5 mM glucose, 2 mM fucose, and 2% dialyzed FCS and then incubated for 30 min in the same medium containing either 100 μCi/ml [2-^{3}H]mannose or 100 μCi/ml [6-^{3}H]glucosamine, respectively. For $Glc_{3\text{-}0}$[^{3}H]$Man_5GlcNAc_2$-PP-dolichol: 8×10^7 Thy^{-1} cells were harvested and then rinsed with glucose-free RPMI 1640 medium containing 0.5 mM glucose, 2.0 mM fucose, and 2% dialyzed FCS and then incubated in 1 ml of the same medium containing 100 μCi [2-^{3}H]mannose for 30 min. $Glc_{3\text{-}0}Man_{9\text{-}8}GlcNAc_2$-PP-[^{3}H]dolichol was generated by cultivating HepG2 cells in normal growth medium containing 10 μM mevinolin and 100 μCi/ml [5-^{3}H]mevanolactone for 47 h.

Recovery of DLO from radiolabeled cells

These methods are based on previously described procedures (25–27). Washed cells were suspended in 4 ml of methanol/100 mM Tris HCl (pH 7.4) containing 4 mM $MgCl_2$, 2:1. Four milliliters of $CHCl_3$ was added, and the mixture shaken. After centrifugation, DLO was recovered from the lower $CHCl_3$ phase from the $CHCl_3$/methanol/water 10:10:3 extracts of the interphase proteins. These DLO preparations were kept at −20°C until required. Where indicated, oligosaccharides were released from DLO after mild acid hydrolysis with 0.02 N HCl for 30 min at 100°C.

Preparation of total cell membranes

Seventy percent to 100% confluent HepG2 cell monolayers were rinsed and scraped into PBS. Pelleted cells were taken up in 10 mM Tris/HCl pH 7.4 containing protease inhibitors. After 20 min, cells were homogenized in the same buffer using a Dounce homogenizer, and postnuclear supernatants were then centrifuged at 100,000 g_{Av} for 35 min. The pellets were taken up in 100 mM Tris/HCl pH 7.4 containing protease inhibitors, aliquoted, and frozen at −80°C.

Differential centrifugation of mouse liver homogenates

Livers from fasted C57BL6J mice were homogenized and fractionated according to a protocol devised for rat liver (28). The mice were euthanized by cervical dislocation in accordance with the Debré-Bichat Ethics Committee on Animal Experimentation Protocol Number 2012-15/773-0091 and in accordance with French law on the protection of animals. Livers were removed,

weighed, and transferred to ice-cold homogenization buffer (HB: 10 mM HEPES/NaOH pH 7.4 containing 250 mM sucrose, 1 mM EDTA, and protease inhibitors). The livers were cut into small pieces, rinsed with HB, and homogenized with 10 strokes in a Potter-Elvehjem homogenizer (800 rpm) with 4 vol of HB. In some experiments, a loose-fitting Dounce apparatus was used to homogenize the tissue. Homogenates were centrifuged at 750 g_{Av} for 5 min, 2,500 g_{Av} for 10 min, 12,500 g_{Av} for 10 min, and 100,000 g_{Av} for 45 min to give P1, P2, P3, and P4, respectively, and a final supernatant (S). Pellets and supernatant were aliquoted and frozen at −80°C.

Optiprep density gradient fractionation of mouse liver microsomes

Mouse liver P4 was prepared as described above with exception that EDTA was omitted from the HB. Optiprep solutions were diluted into 10 mM HEPES/NaOH pH 7.40, containing 250 mM sucrose. Mouse liver P4 was centrifuged at 350,000 g_{Av} for 90 min on the Optiprep gradient described in (29) using a Beckman VTi 65.2 rotor.

Enzyme assays

Protein and enzymes were detected using the following methods: protein BCA reagent (30), lactate dehydrogenase (31), citrate synthase (32), phosphodiesterase I (33), acid phosphatase (34), UDP-galactose glycoprotein galactosyltransferase (UGT) (35), dolichyl-P-mannose synthase (DPMS) (36), dolichyl-P-glucose synthase (DPGS) (37), NADPH cytochrome c reductase (NCCR) (38). UDP-GlcNAc-DolP-GlcNAc 1-P phosphotransferase (DPAGT) (39).

Western-blot analysis

Samples prepared from density gradient fractions were diluted to the same protein concentration, heated with NuPAGE LDS sample buffer under reducing conditions according to the manufacturer's instructions, and subjected to SDS-PAGE; the primary antibodies were detected using horseradish-peroxidase-coupled secondary antibodies.

Standard DLODP assay

Metabolically radiolabeled DLO (3×10^{-3} to 50×10^{-3} cpm) was dried down into 1.5 ml centrifuge tubes before being resuspended in 5 μl 1% NP-40. Further components were added to give final 50 μl reaction mixtures containing 100 mM MES, pH 5.5, 1 mM $CoCl_2$, 0.1% NP-40, and various quantities of membrane protein that are indicated in the figure legends. Incubations were carried out at 37°C for various times, as indicated in the figure legends, and stopped by the addition of 150 μl ice-cold 10 mM $MgCl_2$, 400 μl ice-cold methanol and 600 μl $CHCl_3$ (25). After vigorous shaking, the phases were separated as described above, and after removal of organic solvent, the radioactivity associated with the $CHCl_3$ phase was assayed by scintillation counting (cpm DLO). The upper phase was dried down under vacuum and loaded onto coupled 500 μl Dowex 50WX2 (H^+ form) and Dowex 1 × 2 (acetate form) ion-exchange columns in water. The eluate and water washes containing neutral radioactive components were dried under vacuum and assayed by scintillation counting. The Dowex 1 × 2 (acetate form) columns were eluted with 5 ml 3.0 M formic acid, and after drying under vacuum, negatively charged components were assayed by scintillation counting (cpm formic acid). DLODP activity is defined as cpm formic acid/(cpm DLO + cpm formic acid). Percent inhibition of DLODP activity is defined as $100 - (100 \times \text{DLODP activity}_{+\text{inhibitor}}/\text{DLODP activity}_{\text{control}})$.

Analytical procedures

Where indicated, after desalting on Biogel P2 columns, charged oligosaccharides were fractionated on quaternary aminoethyl (QAE)-Sephadex columns (40) as previously described (11). DLOs were chromatographed on 4 ml DE-52 cellulose (acetate form) columns (41) and eluted with 6 vol of $CHCl_3$/methanol/water (10:10:3), 6 vol of $CHCl_3$/methanol/5 mM ammonium acetate (10:10:3), and finally, 6 vol of $CHCl_3$/methanol/100 mM ammonium acetate (10:10:3). Neutral oligosaccharides were separated on silica-coated plastic sheets (0.2 mm thickness) developed in *n*-propanol-acetic acid-water (3:3:2) for 16–24 h (TLC system 1) (41). Dolichol and DolP were resolved on prerun silica-coated aluminum sheets (0.2 mm thickness) developed in $CHCl_3$/methanol/NH_4OH (65:35:5) for 1 h (TLC system 2). DLOs were separated on prerun silica-coated aluminum sheets (0.2 mm thickness) in $CHCl_3$/methanol/water (10:10:3) for 5 h (TLC system 3) (42). Mono-, di-, tri-, and tetra-saccharides were separated on cellulose-coated plastic sheets developed in pyridine-ethyl acetate-water-acetic acid (5:5:3:1) for 16 h (TLC system 4). Radioactive components were detected on X-OMAT AR film by fluorography after spraying the dried TLC plates with En^{3}hance and were quantitated by scintillation counting after their elution with water from the silica. Compounds containing terminal nonreducing GlcNAc residues were quantitated by transferring [^{3}H]galactose from UDP-[^{3}H]galactose using bovine milk galactosyltransferase as previously described (43).

RESULTS

Detergent, ion, and pH requirements for OSP generation by total HepG2 membranes

Cells from various mammalian sources contain a detergent- and Mn^{2+}-requiring activity that generates OSP from DLO (12, 26, 44, 45). In preliminary experiments, we confirmed the presence of this activity in human hepatocellular carcinoma HepG2 cell total membrane preparations. In incubation mixtures containing 100 mM Tris HCl, pH 7.5, 0.5% w/v Triton X-100, and 1 mM $MnCl_2$, this activity hydrolyzes both truncated ($Man_7GlcNAc_2$-PP-dolichol) and mature ($Glc_{3\text{-}0}$[2-^{3}H]$Man_9GlcNAc_2$-PP-dolichol) DLO (A. Massarweh and S.E.H. Moore, unpublished observations). DLO hydrolysis conditions were reevaluated because DLO hydrolysis required large amounts of protein and long incubation times. To do this, HepG2 membranes were incubated with $Glc_{3\text{-}0}$[2-^{3}H]$Man_9GlcNAc_2$-PP-dolichol in a reaction mixture containing 100 mM Tris HCl, pH 7.5, 0.5% w\v Triton X-100 and various cations at a final concentration of 10 mM. After stopping the reactions, solvent extractions were performed and radioactivity associated with DLO, protein, OSP, and nfOS plus other neutral sugar (nfOS/S) was quantitated (see **Fig. 1A** for workup scheme). When reaction mixtures are supplemented with Co^{2+}, Mn^{2+}, or Ni^{2+}, DLO is lost with a concomitant increase in OSP (Fig. 1B). To optimize detergent and pH conditions for OSP generation, Co^{2+} was used to promote DLO cleavage. OSP generation requires detergent, and the three neutral detergent preparations Triton X-100, NP-40, and IGEPAL have similar capacities to promote this process (Fig. 1C). Further studies were carried out using 0.1% NP-40. The reaction has a pH optimum of 5.5 and is more efficient in HEPES, MOPS, and MES buffers than in Tris, pyridine, or propionate buffers (Fig. 1D). Finally, the divalent cation requirement for the reaction was reevaluated in the presence

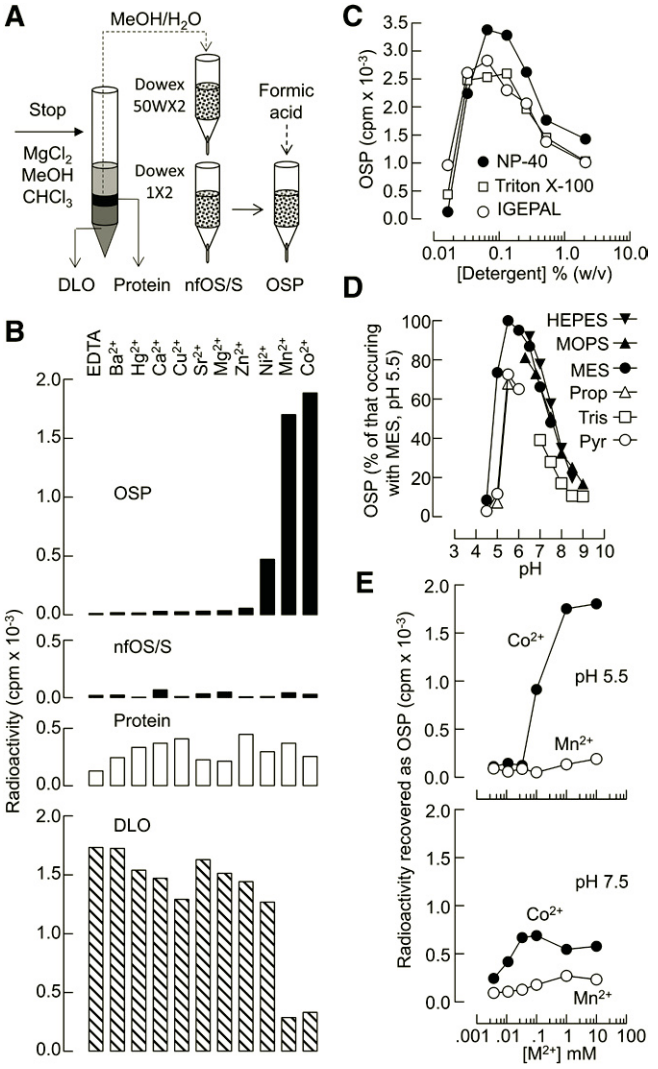

Fig. 1. Optimization of incubation conditions for release of OSP from DLO by HepG2 membranes. A: Assay workup. The 50 µl reactions were stopped by the addition of 150 µl 10 mM $MgCl_2$, 400 µl methanol, and 600 µl $CHCl_3$. After shaking, the different phases were separated and dried down under vacuum. DLOs were recovered from the lower $CHCl_3$ phase and directly assayed by scintillation counting. The interphase material containing precipitated protein was solubilized with pronase and assayed by scintillation counting (Protein). The upper methanol-water phase was desalted on Dowex 50WX2/Dowex 1 × 2 ion-exchange columns. Neutral components comprising nfOS and monosaccharides (nfOS/S) were dried under vacuum and assayed by scintillation counting. The 3M formic acid eluates of the Dowex 1 × 2 columns were dried down under vacuum and assayed by scintillation counting (OSP). B: $Glc_{3\text{-}0}[^3H]Man_9GlcNAc_2$-PP-dolichol was incubated with 107 µg HepG2 cell membrane protein in the presence of 0.5% w/v Triton X-100, 10 mM of the indicated cations or EDTA, and 100 mM Tris/HCl pH 7.5 for 4 h at 37°C, and radioactivity in the fractions (defined in A) was assayed by scintillation counting. C: $Glc_{3\text{-}0}[^3H]Man_9GlcNAc_2$-PP-dolichol was dried down into tubes and suspended in different quantities of detergents to give the final concentrations indicated. Incubations were conducted in the presence of 43 µg HepG2 cell membranes protein, 1 mM $CoCl_2$, and 100 mM Tris/HCl buffer, pH 7.5, for 2 h at 37°C. Fractions were worked up as in A, and the radioactivity associated with OSP was assayed by scintillation counting. D: In several different experiments, $Glc_{3\text{-}0}[^3H]Man_9GlcNAc_2$-PP-dolichol was incubated for 45 min at 37°C with 18 µg HepG2 cell membranes in the presence of 0.1% w/v NP-40, of 0.1% NP-40 and 100 mM MES buffer at both pH 5.5 and pH 7.5 (Fig. 1E). When the concentrations of Co^{2+} and Mn^{2+} were varied at pH 5.5, it was noted that even 10 mM Mn^{2+} possessed little capacity to provoke OSP generation, whereas 1 mM Co^{2+} was sufficient to elicit maximal activity. At pH 7.5, the maximal activation seen with Co^{2+} was lower than that noted at pH 5.5, but this cation appeared to be able to promote DLO cleavage at lower concentrations than at pH 5.5. As indicated in the legend to Fig. 1, the modifications made to the incubation conditions, from Fig. 1B to Fig. 1E, allowed reductions of both the amount of protein required and the assay incubation time. The standard conditions for further exploration of DLO cleavage were 0.1% NP-40, 100 mM MES, pH 5.5, and 1 mM Co^{2+}.

Characterization of DLO and OSP glycan moieties during standard incubation conditions

As shown in **Fig. 2A**, a time-dependent decrease in $Glc_{3\text{-}0}[2\text{-}^3H]Man_9GlcNAc_2$-PP-dolichol is accompanied by an increase of OSP. It was noted, though, that total recovery of radioactivity from the different fractions was low at the zero and early time points (Fig. 2A). Experiments revealed that this was because $Glc_{3\text{-}0}[2\text{-}^3H]Man_9GlcNAc_2$-PP-dolichol partitions poorly into the $CHCl_3$ phase (see Fig. 1A) during the solvent extraction of the standard reaction mixtures and is lost during workup of the methanol-water phase (Fig. 2B). Addition of the ER glucosidase I/II inhibitor Cst and the ER/Golgi mannosidase I inhibitor Kif, as well as the Golgi mannosidase II/lysosomal/cytosolic mannosidase inhibitor Sw, to the standard incubation mixtures demonstrate that the glycan moieties of both the released OSP and substrate DLO are processed by glycosidases (Fig. 2C). As the profile of released OSP generated during mannosidase and glucosidase blockade is still different from that of glycans derived from the starting DLO, it can be concluded that inhibitor-insensitive glycosidases are active under these incubation conditions.

Assays using the truncated $Glc_{3\text{-}0}[2\text{-}^3H]Man_5GlcNAc_2$-PP-dolichol substrate revealed that radioactivity was rapidly lost from DLO and concomitantly associates with both the nfOS/S and OSP fractions (Fig. 2D). By contrast to results reported above, the use of this truncated DLO substrate led to the recovery of a constant sum of radioactivity (*Total*, Fig. 2D) from the different incubations, perhaps due to better partitioning of the smaller DLO structures into the $CHCl_3$ phase after solvent extraction. Addition of the mannosidase inhibitors to the incubations led to a

1 mM $CoCl_2$, and the indicated buffers at a concentration of 100 mM. Fractions were worked up as in A, and results are presented as the quantity of OSP recovered compared with that recovered with the MES buffer, pH 5.5, which was used in each experiment as a reference. Prop, propanoic acid; Pyr, pyridine. E: $Glc_{3\text{-}0}[^3H]Man_9GlcNAc_2$-PP-dolichol was incubated with 16.6 µg HepG2 cell membranes in the presence of 0.1% w/v NP-40, 100 mM MES, pH 5.5 or pH 7.5, containing the indicated concentrations of Co^{2+} or Mn^{2+} for 25 min at 37°C. Fractions were worked up as in A, and OSPs were quantitated by scintillation counting. Data presented in B–E are from single experiments.

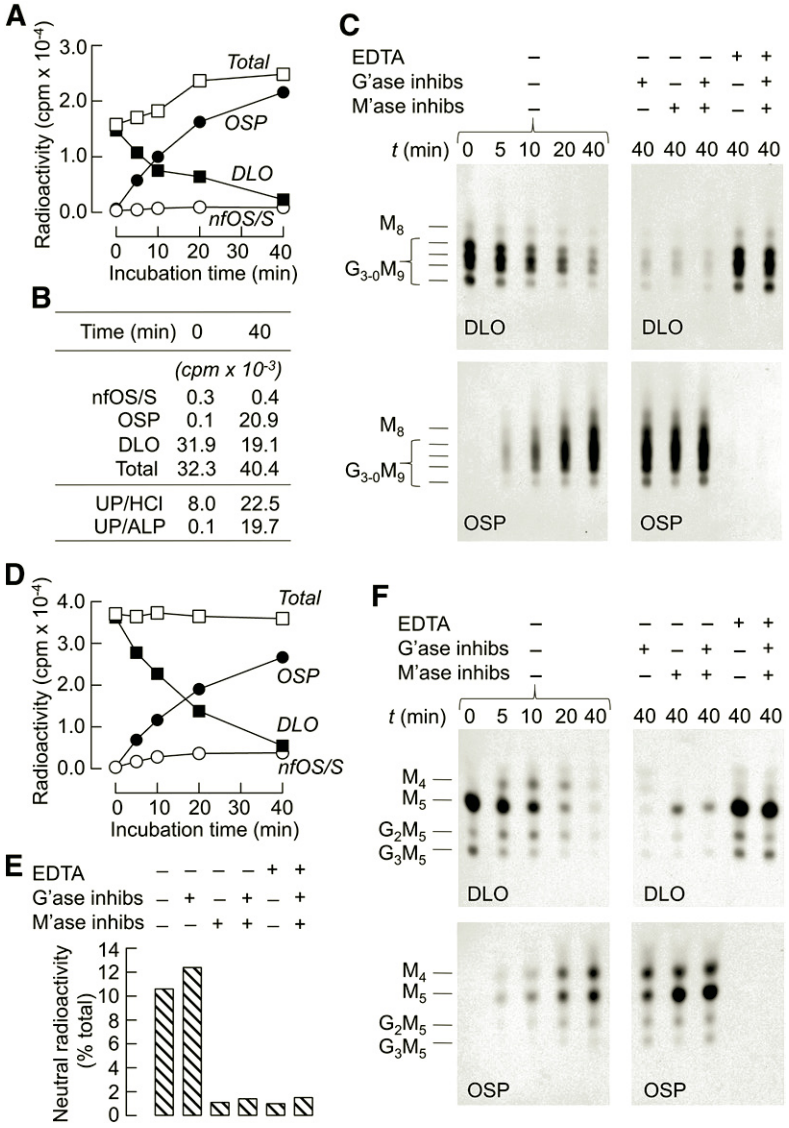

Fig. 2. Characterization of the reaction products generated during incubation of DLO under standard incubation conditions. A: $Glc_{3\text{-}0}Man_9GlcNAc_2$-PP-dolichol was incubated with 23.3 μg HepG2 cell membranes for the indicated times. Additional 40 min time point incubation mixtures were supplemented with the glucosidase inhibitors Cst (1 mM) and deoxynojirimycin (1 mM) (G'ase inhibs) or the mannosidase inhibitors Kif (100 μM) and Sw (100 μM) (M'ase inhibs) as indicated. Cobalt was not added to the incubations that were supplemented with 1 mM EDTA. After stopping the reactions and workup of samples as described in the legend of Fig. 1A, radioactivity associated with the $CHCl_3$ phase (*DLO*), methanol/water-soluble neutral (*nfOS/S*), and negatively charged (*OSP*) material was quantitated by scintillation counting. The three values obtained for each time point were summed to give the total radioactivity recovered from the incubation (*Total*). B: In a similar experiment, the zero and 40 min time point incubations were analyzed as described above to yield radioactivity associated with nfOS/S, OSP, DLO, and total fractions. In duplicate incubations, the methanol/water upper phase was dried down and loaded onto Dowex 50WX2/Dowex 1 × 2 columns after either no treatment, hydrolysis with 20 mM HCl, or digestion with ALP. Radioactivity passing through the columns was assayed by scintillation counting, and the radioactivity found in the control samples (no treatment) was subtracted from the values found for the HCl- and ALP-treated samples to yield the amount of radioactivity neutralized by HCl (UP/HCl) and ALP (UP/ALP). C: Substrate DLO and product OSP recovered from the experiment described in A were hydrolyzed with 20 mM HCl, and the resulting neutralized oligosaccharides were resolved using TLC system 1. The migration positions of $Glc_3Man_9GlcNAc_2$ (G_3M_9), $Glc_2Man_9GlcNAc_2$ (G_2M_9), $Glc_1Man_9GlcNAc_2$ (G_1M_9), $Man_9GlcNAc_2$ (M_9), and $Man_8GlcNAc_2$ (M_8) are indicated to the left of the chromatograms. D, F: The experiment described in A and C was repeated using $Glc_{3\text{-}0}Man_5GlcNAc_2$-PP-dolichol as substrate. The migration positions of $Glc_3Man_5GlcNAc_2$ (G_3M_5), $Glc_2Man_5GlcNAc_2$ (G_2M_5), $Man_5GlcNAc_2$ (M_5), and $Man_4GlcNAc_2$ (M_4) are indicated to the left of the chromatograms. E: Radioactivity associated with nfOS/S fraction is expressed as a percentage of the total radioactivity recovered in the 40 min incubations of D and F. The data shown in A–F are from single experiments.

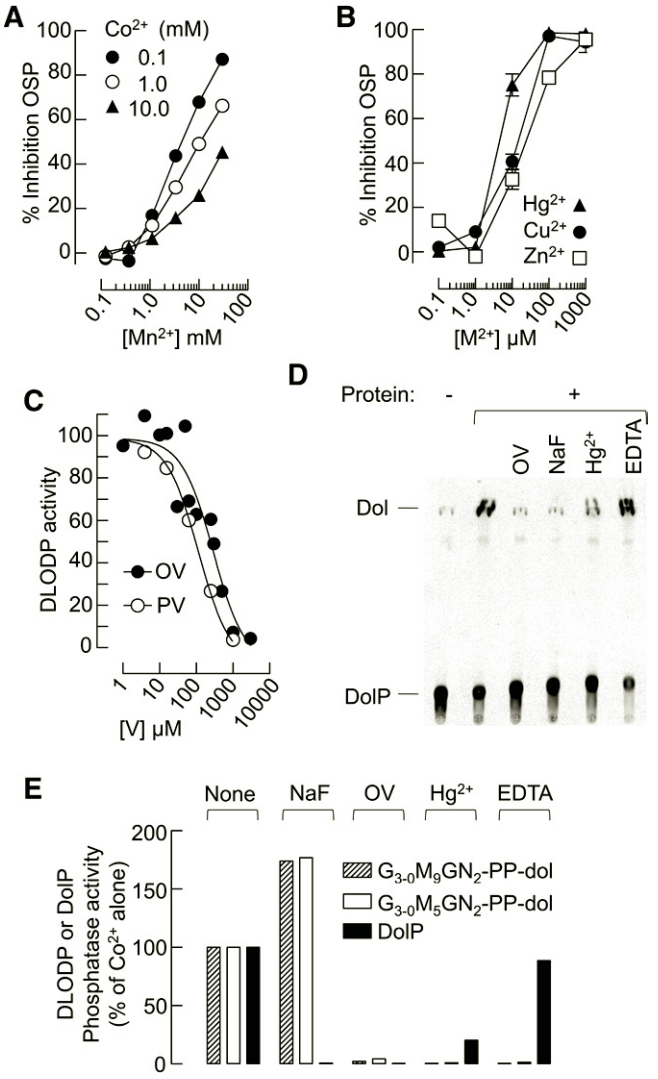

Fig. 3. Inhibitor profiling of OSP generation and DolP dephosphorylation. A: Inhibition of Co^{2+}-elicited OSP generation by Mn^{2+} ions was measured in the presence of different concentrations of Co^{2+} during 25 min incubations with 20 µg HepG2 cell membrane proteins. B: Inhibition of Co^{2+}-elicited OSP generation by the indicated divalent cations was measured in the presence of 1 mM Co^{2+} during 25 min incubations with 20 µg HepG2 cell membrane proteins. The data points for the three highest concentrations for each ion were performed in duplicate, and the error bars represent the standard error of the mean. C: In three separate experiments, 25 min incubations with 20 µg HepG2 cell membrane proteins were conducted in the presence of sodium orthovanadate (OV) or sodium pervanadate (PV) that was produced by treating OV with H_2O_2 for 15 min followed by elimination of excess H_2O_2 with catalase (67). D: [^{3}H]DolP was incubated with 23 µg HepG2 cell membrane proteins for 30 min under the standard DLO hydrolysis mixture supplemented with either 5 mM OV, 50 mM NaF, 100 µM Hg^{2+}, or 10 mM EDTA. As a negative control, an incubation without enzyme source was performed. The reactions were stopped and extracted with organic solvents as shown in Fig. 1A. The $CHCl_3$ phase was dried and analyzed using TLC system 2. The migration positions of standard dolichol (Dol) and DolP are indicated to the left of the chromatogram. E: After elution of the Dol and DolP from the TLC plate shown in D and quantitation by scintillation counting, DolP phosphatase activity was defined as [^{3}H]Dol/([^{3}H]DolP + [^{3}H]Dol). In the same experiment, the cleavage of either $Glc_{3\text{-}0}Man_9GlcNAc_2$-PP-dolichol or $Glc_{3\text{-}0}Man_5GlcNAc_2$-PP-dolichol was measured. For all substrates, activity is expressed as percent change with respect to that seen without inhibitors (none: set at 100%). Apart from the experiment shown in B, the data shown are from single experiments.

striking decrease in radioactivity associated with the nfOS/S fraction indicating that [2-^{3}H]mannose is liberated from the substrates and/or reaction products by mannosidases (Fig. 2E). This was confirmed after acid hydrolysis of both the DLO and OSP material recovered from the methanol/water-soluble fraction, and subsequent resolution of the oligosaccharide products by TLC (Fig. 2F). First, as shown in the left-hand panels, DLO (upper panel) is cleaved to yield OSP (lower panel) in a time-dependent manner. Second, both DLO and the OSP are degraded by glycosidases. The right-hand panels of Fig. 2F demonstrate that, unlike the formation of the $Man_4GlcNAc$ OSP structure, glycosidase inhibitors block trimming of DLO. To summarize, these data demonstrate that both DLO and OSP are deglucosylated and demannosylated during the standard reaction conditions, and to minimize these unwanted side reactions, all further incubations were carried out in the presence of the glycosidase inhibitors Sw, Kif, and Cst. Furthermore, because of the improved recoveries of the truncated DLO substrates during the reaction workup procedure, $Glc_{3\text{-}0}$[2-^{3}H]$Man_5GlcNAc_2$-PP-dolichol was used as the standard reaction substrate unless otherwise stated.

Comparison of the OSP-generating activity with DolP and DolPP phosphatase activities

Mammalian cells contain lipid phosphate phosphatases with broad substrate specificities that can cleave, for example, the phosphate linkages in DolPP and DolP (46, 47), and one or more could hydrolyze DLO to yield either DolP and OSP or OSPP and Dol. In the latter case, OSPP could be rapidly dephosphorylated to yield OSP. To address this question, we compared the susceptibility of the OSP-generating activity with agents that are known to affect DolP and DolPP dephosphorylation. First, DolPP hydrolysis by brain and liver enzymes is inhibited by Mn^{2+} and activated by EDTA (47, 48). Data presented in **Fig. 3A** show that Mn^{2+} inhibits Co^{2+}-dependent OSP release from DLO in a Co^{2+}-dependent manner, suggesting that these two ions compete for the same role during the hydrolysis reaction. Nevertheless, taking into account that DolPP phosphatase activities are cation independent and activated by EDTA, it seems unlikely that they could account for the Co^{2+}-activated OSP-generating mechanism described here. Second, like the DolPP phosphatase activities, brain and liver DolP phosphatase are cation independent, but unlike the former activities, are inhibited by NaF (47, 49). As NaF activates OSP liberation from DLO (see below), it is again unlikely that the previously described liver DolP phosphatases could participate in the OSP-generating process described here. While further profiling the OSP-generating activity, it was noted that Hg^{2+}, Cu^{2+}, and Zn^{2+} inhibit OSP generation, indicating that a cysteine residue is important for the reaction (Fig. 3B). The phosphatase inhibitors orthovanadate and pervanadate also block OSP generation (Fig. 3C). Next,

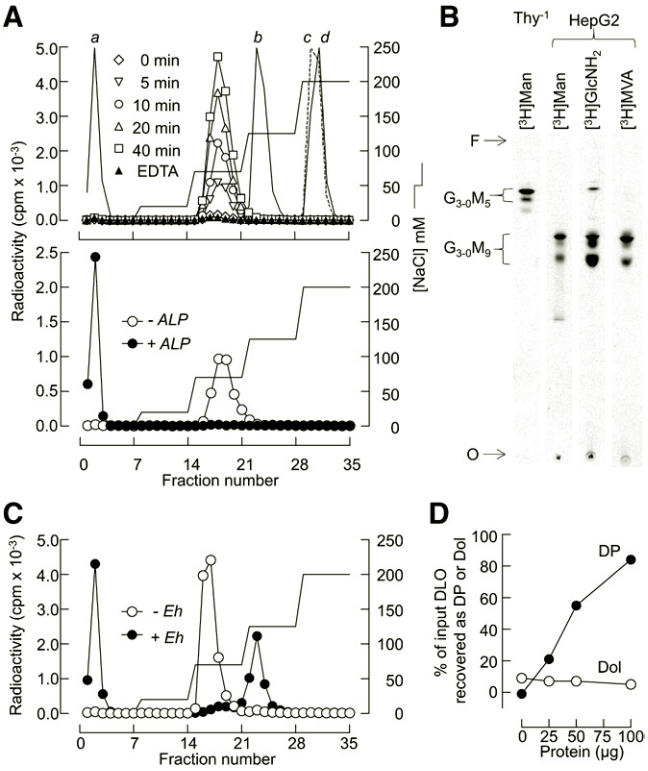

Fig. 4. Characterization of the charge of the reaction products generated from DLO under standard incubation conditions. A: Upper panel: $Glc_{3\text{-}0}[^3H]Man_5GlcNAc_2$-PP-dolichol was incubated under the standard reaction conditions in the presence of both the mannosidase and glucosidase inhibitors for the indicated times exactly as described for Fig. 2. OSP were desalted on Biogel P2 columns and taken to dryness before loading onto QAE-Sephadex ion-exchange columns in 2 mM Tris base. Step-wise elution of components was achieved with 2 mM Tris base containing the indicated concentrations of NaCl. The column was calibrated with the following: *a*, $[^3H]Gal\beta1,4GlcNAc_2$; *b*, [^{3}H]glucose-1-phosphate; *c*, UDP-[^{3}H]*N*-acetylglucosamine; *d*, [^{14}C]isopentenyl pyrophosphate. Lower panel: Aliquots of the desalted negatively charged water-soluble products obtained from the 40 min incubation were incubated in either the presence or absence of ALP prior to being loaded onto QAE-Sephadex ion-exchange columns as described above. B: DLO obtained from HepG2 cells (HepG2) or DPMS-deficient (Thy^{-1}) lymphoma cells that were metabolically radiolabeled with [2-^{3}H]mannose ([^{3}H]Man) and DLO derived from HepG2 cells that were metabolically radiolabeled with either [6-^{3}H]glucosamine ($[^3H]GlcNH_2$) or [5-^{3}H]mevanolactone ([5-^{3}H]MVA) were analyzed using TLC system 3. O, origin; F, solvent front; $G_{3\text{-}0}M_5$, $Glc_{3\text{-}0}Man_5GlcNAc_2$-PP-dolichol; $G_{3\text{-}0}M_9$, $Glc_{3\text{-}0}Man_9GlcNAc_2$-PP-dolichol. C: $Glc_{3\text{-}0}Man_9[^3H]GlcNAc_2$-PP-dolichol was prepared as described in Materials and Methods and incubated under standard conditions for 40 min, and aliquots of the desalted OSP were incubated in either the absence or presence of *S. plicatus* endo H (*Eh*) prior to being fractionated on QAE-Sephadex ion-exchange columns as described above. D: $Glc_{3\text{-}0}Man_9GlcNAc_2$-PP-[^{3}H]dolichol was incubated for 40 min in the standard incubation mixture, supplemented with 50 mM NaF, with the indicated amounts of HepG2 membrane protein. After stopping the reactions as described for Fig. 1A, the $CHCl_3$ phase was washed with practical upper phase, dried down, and subjected to DE-52 anion-exchange chromatography as described in Materials and Methods. Radioactivity associated with the unbound fraction [where standard dolichol (Dol) elutes] and that eluted with $CHCl_3$/methanol/5 mM ammonium acetate (10:10:3) (where standard DolP elutes) was quantitated by scintillation counting after removal of solvents. The increase in radioactivity associated with each fraction is expressed as percentage of the amount of radioactive DLO initially taken for digestion. Although detected, radioactivity associated with DLO in the $CHCl_3$ phase after solvent extraction of the reaction mixtures was lower than expected, probably for reasons discussed in Fig. 2A, B. The data shown in all the panels are from single experiments.

because DolP dephosphorylation is normally assayed in the absence of cations and at pH 7.5, we examined the effects of vanadate, NaF, Hg^{2+}, and EDTA on DolP dephosphorylation under the standard assay conditions used for releasing OSP from DLO. Under these conditions, only EDTA did not inhibit DolP dephosphorylation (Fig. 3D). To summarize (Fig. 3E), we established a reaction condition (+ NaF) where DolP dephosphorylation is blocked but OSP liberation from DLO (both mature and truncated DLO) continues. However, as NaF did not block the dephosphorylation of DolPP under these reaction conditions (results not shown), we could not identify a condition where OSP generation from DLO occurs in the absence of DolPP dephosphorylation. These results demonstrate that, although OSP generation from DLO is carried out by an activity, or activities, distinct from previously characterized DolP and DolPP phosphatases, the possibility that the OSP-generating enzyme can also dephosphorylate DolPP cannot be excluded.

The OSP-generating activity is a diphosphatase

The liberation of OSP from DLO could occur by either splitting of the diphosphate linkage by a diphosphatase or initial cleavage of the DolP linkage by a phospholipase-like enzyme followed by rapid conversion of OSPP to OSP (15). In order to look for a putative OSPP, $Glc_{3\text{-}0}[2\text{-}^3H]Man_5GlcNAc_2$-PP-dolichol was incubated with HepG2 membranes under standard conditions in the presence of mannosidase and glucosidase inhibitors as described for Fig. 2, and after desalting on Biogel P2 columns, the anionic methanol/water reaction products were subjected to anion exchange chromatography on QAE-Sephadex. The chromatograph shown in **Fig. 4A** (upper panel) demonstrates that whatever the incubation time the anionic material is predominantly eluted from the columns with 75 mM NaCl: similarly to OSP isolated from intact cells, and as expected, ALP treatment of the anionic material yields a neutral oligosaccharide (Fig. 4A, lower panel). In order to investigate the difference in apparent charge of OSP and glucose-1P during QAE-Sephadex chromatography (Fig. 4A, upper panel), $Glc_{3\text{-}0}Man_9[^3H]GlcNAc_2$-PP-dolichol (Fig. 4B, lane $[^3H]GlcNH_2$) was incubated with total HepG2 membranes under the standard conditions. Aliquots of the desalted water-soluble product were then treated either with *S. plicatus* endo H or incubation buffer alone. After desalting, the reaction products were subjected to anion exchange chromatography, and it can be seen that endo H treatment gives rise to a neutral compound and another, possessing a higher apparent charge than OSP, which coeluted with glucose-1P (Fig. 4C). These data are consistent with $Glc_{3\text{-}0}Man_9[^3H]GlcNAc_2$-P being hydrolyzed by endo H to yield $Glc_{3\text{-}0}Man_9[^3H]GlcNAc$ and $[^3H]GlcNAc$-1P and

demonstrate that under our standard assay conditions DLOs are hydrolyzed to yield products with the characteristics of the OSP that have been previously isolated from intact cells. Therefore, either an OSPP intermediate is too short lived to be detected, or a diphosphatase reaction mechanism is involved. The distinguishing feature of the diphosphatase mechanism is the production of DolP, whereas that of the mechanism yielding OSPP as an intermediate is the production of dolichol. Accordingly, $Glc_{3\text{-}0}Man_9GlcNAc_2$-PP-[^{3}H]dolichol (Fig. 3B, lane [^{3}H]MVA) was incubated with increasing amounts of total HepG2 membrane protein in the standard incubation mixture supplemented with 50 mM NaF in order to block dephosphorylation of any released [^{3}H]DolP (see above). A protein-dependent generation of a charged [^{3}H]lipid component that coelutes with standard [^{3}H]DolP during DEAE-cellulose chromatography was noted (Fig. 3D). In fact, >80% of the input $Glc_{3\text{-}0}Man_9GlcNAc_2$-PP-[^{3}H]dolichol was recovered as [^{3}H]DolP. By contrast, no evidence was obtained for the generation of [^{3}H]dolichol during the reactions. Therefore, under our standard reaction conditions, DLODP activity liberates OSP and DolP from DLO.

DLODP activity is inhibited by lipophilic phospho compounds

To evaluate potential physiological substrates for the DLODP activity, various water-soluble mono-, di-, and triphospho compounds were tested to find out whether they interfered with the liberation of [^{3}H]OSP from [^{3}H]DLO. At a concentration of 3 mM (75,000-fold excess over [^{3}H]DLO substrate), ATP, ADP, AMP, UDP, UMP, UDP-GlcNAc, UDP-Gal, NADPH, Glc-1P, Man-1P, and Man-6P inhibited DLO action by <50%. The lipophilic compounds phosphatidic acid (PA; IC_{50} >100 μM), diacylglycerol diphosphate (DGPP; IC_{50} >100 μM), lysophosphatidic acid (LPA; IC_{50} 9 μM), and DolP (IC_{50} 7 μM) inhibited the reaction at lower concentrations than the water-soluble compounds, but sphingosine-1P possessed no inhibitory activity at a concentration of 300 μM. Next, we took a systematic approach to identifying potential physiological substrates for DLODP. First, a series of compounds comprising commercially available, as well chemically synthesized, isoprenoid diphosphates with differing alkyl chain lengths was tested for DLODP assay inhibition (**Fig. 5A**). As shown in Fig. 5B, there is a good correlation between alkyl chain length between 5 and 20 carbons and reaction inhibition, whereas a further increase in the chain length from 20 to 45 carbons produced a less striking effect. Comparison of the IC_{50} value obtained for citronellyl diphosphate, a compound whose structure is identical to the first 10 carbon residues of DolPP (Fig. 5A), with that obtained for geranyl diphosphate indicates that, at least for these short chain compounds, the structure of the alkyl chain is not a critical factor for inhibition of DLODP activity (Fig. 5B).

Lipophilic diphosphodiesters inhibit DLODP activity more effectively than lipophilic diphosphomonoesters

As mentioned earlier, we were unable to identify reaction conditions where DolPP is not dephosphorylated

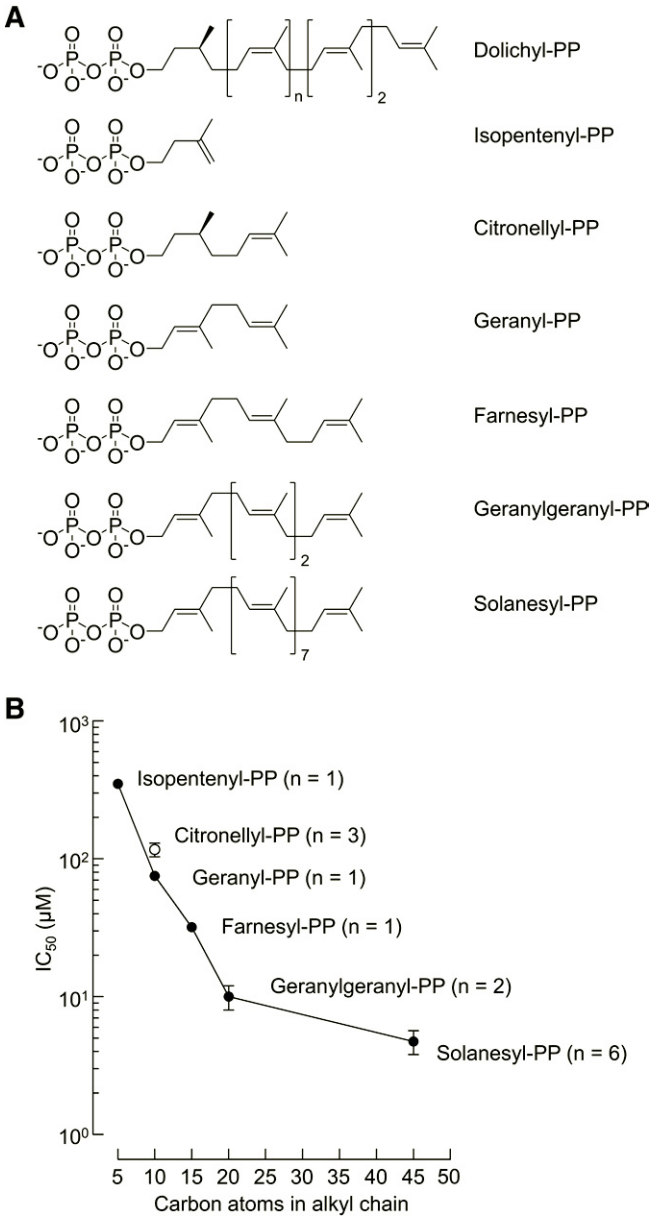

Fig. 5. Inhibition of DLODP activity by different isoprenoid diphosphates. A: Standard DLODP reaction mixtures containing 40 nM $Glc_{3\text{-}0}$[^{3}H]$Man_5GlcNAc_2$-PP-dolichol, 21 μg HepG2 cell membrane protein, and different concentrations of the indicated isoprenoid diphosphates were incubated for 20 min at 37°C. The structural relationships between DolPP and the indicated shorter chain isoprenoids are shown. B: Inhibition curves were constructed, and IC_{50} values were determined and plotted as a function of the number of carbon atoms in the isoprenoid moieties. Where IC_{50} values were determined more than once (n > 1), the mean and standard error of the mean are indicated.

and OSP is generated from DLO. So, it is possible that the preferred substrates for DLODP are actually lipophilic diphosphomonoesters like polyprenyl diphosphates. To address this question, a series of compounds, based on the solanesyl moiety (**Fig. 6A**, 1–5), was tested in the DLODP assay. The data demonstrate that the closer the test compound resembles a DLO substrate, the better the inhibition of the reaction. Importantly, the $GlcNAc_{1\text{-}2}$-PP-solanesol compounds inhibited the DLODP assay more efficiently

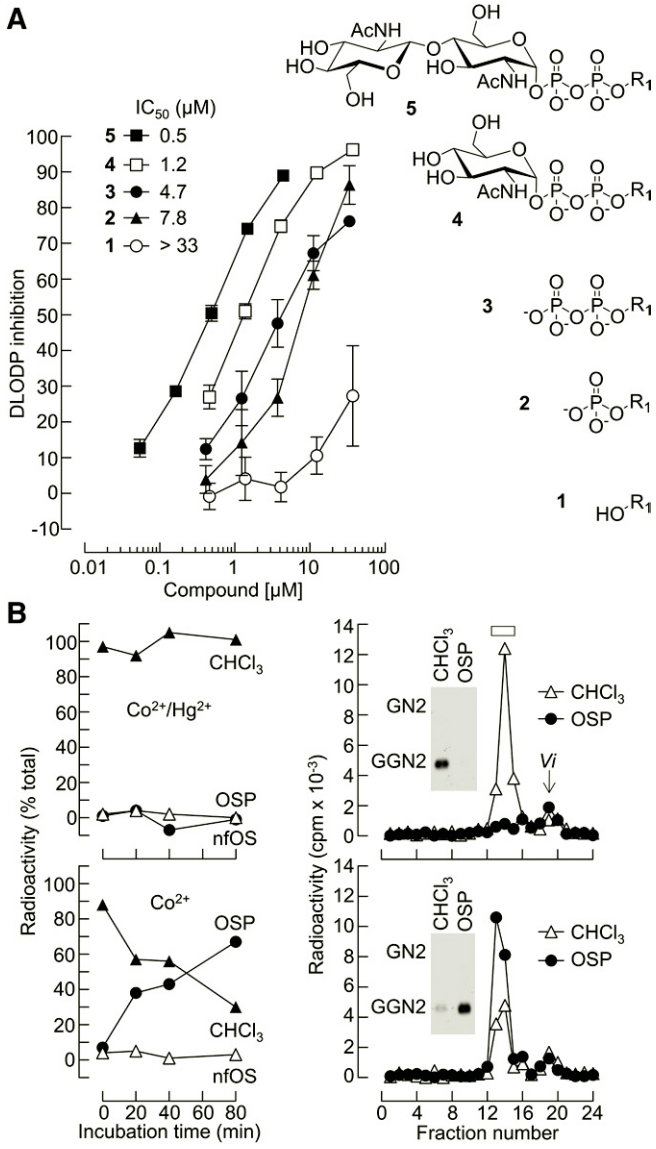

Fig. 6. Inhibition of DLODP activity by solanesyl diphosphomono- and diesters. A: Solanesol (1), P-solanesol (2), PP-solanesol (3), GlcNAc-PP-solanesol (4), and $GlcNAc_2$-PP-solanesol (5) were tested as described in the legend to Fig. 5. Dose-response curves were generated, and the IC_{50} values are reported. Apart from solanesol where n = 2, the dose-response curves were performed at least in triplicate. The mean and standard error of the means are shown. B (left panels): 50 pmol of $GlcNAc_2$-PP-solanesol were incubated under standard DLODP reaction conditions containing 20 μg membrane protein and 50 mM NaF in either the absence (Co^{2+}) or presence (Co^{2+}/Hg^{2+}) of 100 μM Hg^{2+}. After stopping the reactions at the indicated times, the mixtures were worked up as shown in Fig. 1A. Material recovered from the $CHCl_3$ phase and OSP fraction were hydrolyzed with 20 mM HCl, and any resulting neutral "GlcNAc acceptor" compounds were tagged with [^{3}H]galactose and quantitated by scintillation counting as described in Materials and Methods. Background "GlcNAc acceptor" levels were determined by performing incubations without $GlcNAc_2$-PP-solanesol and were subtracted from values obtained when the substrate was present. B (right panels): [^{3}H]galactose-tagged GlcNAc acceptors were resolved by TLC after Biogel P2 chromatography. Material eluting before the total inclusion volume (V_i) of the Biogel P2 column (indicated by the open bar) was pooled and analyzed using TLC system 4. Data shown in B is from a single experiment. The migration positions of $GlcNAc_2$ (GN2) and Galβ1,4$GlcNAc_2$ (GGN2) are shown to the left of the fluorographs.

than solanesyl-PP. Nevertheless, at 0.5 μM, the IC_{50} of the most effective inhibitory reagent, $GlcNAc_2$-PP-solanesol, is still 12.5-fold higher than the [^{3}H]DLO substrate concentration, indicating that other structural motifs are necessary for optimal interaction with DLODP. These data show that solanesyl-based compounds interfere with the liberation of [^{3}H]OSP from [^{3}H]DLO but do not demonstrate that these compounds are actually interacting with the DLODP enzyme. To address this question, $GlcNAc_2$-PP-solanesol was tested as a DLODP substrate, and after fractionation of the incubation mixtures as shown in Fig. 1A, cleavage was followed by UGT-mediated transfer of [^{3}H]Gal from UDP-[^{3}H]Gal onto acceptor structures with terminal nonreducing GlcNAc residues. As shown in Fig. 6B (lower left panel), the time-dependent loss of acceptor material from the $CHCl_3$-phase is coincident with the gain in that associated with water-soluble OSP material. No water-soluble neutral acceptor material was generated during the reaction period. When incubations are carried out in the presence of Co^{2+} and Hg^{2+} (Fig. 6B, upper left panel), both the disappearance of the acceptor material in the $CHCl_3$ phase and the appearance of that associated with the OSP fraction are inhibited. Examination of the UGT reaction products recovered from both the $CHCl_3$ phase and OSP fraction by Biogel P2 chromatography and TLC demonstrate the presence of [^{3}H]Gal$GlcNAc_2$ (Fig. 6B, right-hand panels). These results show that, as well as inhibiting DLODP-mediated [^{3}H]OSP release from [^{3}H]DLO, $GlcNAc_2$-PP-solanesol is itself hydrolyzed.

Subcellular localization of mouse liver DLODP activity

In order to evaluate the subcellular localization of the DLODP activity, mouse liver homogenates were subjected to a classical differential centrifugation procedure (28). Data shown in **Fig. 7** demonstrate that DLODP activity fractionates similarly to the ER marker DPMS and the Golgi apparatus (GA) marker UGT (50), and differently to the mitochondrial (citrate synthase), lysosomal (acid phosphatase), plasma membrane (phosphodiesterase), and cytoplasmic (lactate dehydrogenase) markers. These results demonstrate that DLODP is a microsomal activity. Fractionation of microsomes (P4) on self-forming OptiPrep gradients (29) is shown in **Fig. 8A**. The ER markers NCCR and PDI largely codistribute and show that ER membranes are distributed throughout the gradient with peaks of recovery occurring in fractions 2, 5, and 8. The predominantly rough ER marker CNX (51) has a biphasic distribution and is mainly associated with heavier membranes that are recovered in fraction 10. Approximately 10% of CNX is associated with lighter membranes that are recovered in fractions 4 and 5. By contrast, DLODP-containing membranes largely codistribute with those containing UGT and show highest recoveries in fractions 1 and 2. It is noteworthy that the recoveries of DLODP are somewhat higher than UGT recoveries in fractions 7 and 8. Because DLODP generates DolP that could potentially be utilized physiologically by DPMS, DPGS, and DPAGT, we asked whether these key DLO biosynthesis enzymes colocalize with the DLODP activity. Data reported in the

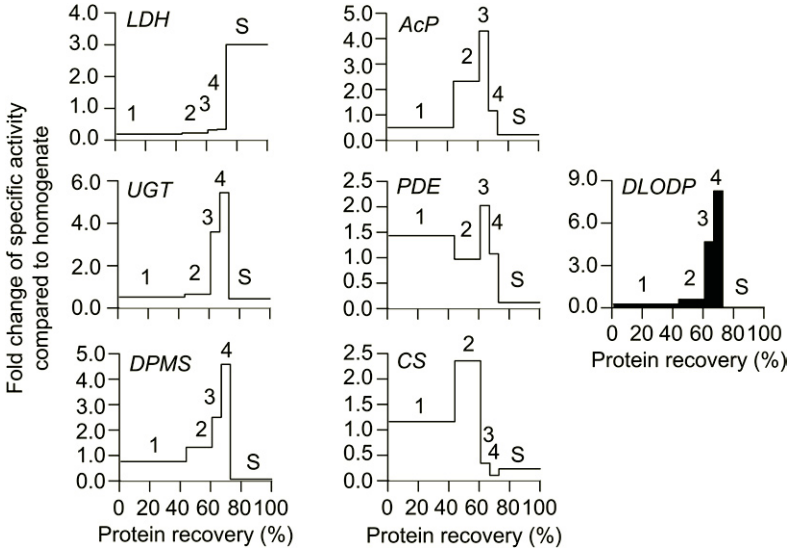

Fig. 7. Subcellular localization of DLODP activity. Mouse liver homogenates were subjected to differential centrifugation as described in Materials and Methods to yield four pellets (1–4) and a final supernatant (S). Along with DLODP, enzyme markers for cytoplasm [lactate dehydrogenase (*LDH*)], microsomes (*UGT* and *DPMS*), lysosomes [acid phosphatase (*AcP*)], plasma membrane [phosphodiesterase (*PDE*)], and mitochondria [citrate synthase (*CS*)] were assayed. The relative enrichments of the specific activities in the various fractions with respect to their specific activities in the initial homogenate are shown. Protein recoveries are expressed as percentages of total protein recovered from P1–4 and S. The data are derived from a single experiment.

lower panel of Fig. 8A demonstrate that the distributions of DPMS, DPGS, and DPAGT are similar to those of the ER markers NCCR and PDI with peaks of recovery in fractions 2, 5, and 8, but different from those of either UGT or DLODP. Data presented in Figs. 7 and 8A were generated using homogenates produced in Potter-Elvehjem apparatus. Homogenization using a Dounce apparatus fitted with a loose pestle is known to generate less shear forces and helps preserve the integrity of intracellular organelles. The gradient fractionation of microsomes (P4) obtained under these milder homogenization conditions is shown in Fig. 8B. Whereas the distributions of membranes containing the ER proteins NCCR, PDI, DPMS, DPGS, and DPAGT are unaffected by the homogenization conditions, the recovery of CNX in light fractions (4, 5) is lost after milder homogenization. The new homogenization conditions also cause subtle changes in the distributions of both DLODP and UGT. Although approximately 50% of both markers are still recovered in fractions containing light membranes (1, 2), they are distributed more equally in these two fractions compared with that seen using the more drastic homogenization conditions. Furthermore, the differences in distributions of UGT- and DLODP-containing membranes in fractions 7 and 8 are now no longer apparent. The ensemble of these results demonstrates that the bulk of DLODP activity shows a similar distribution to that of GA-situated UGT and not those of the ER-situated DolP-dependent enzymes of the dolichol cycle.

DISCUSSION

Progress in our understanding of how and why OSPs are generated has been hampered by the lack of biochemical, cellular, and molecular information on the mechanism of OSP release. An activity that liberates OSP from DLO was first described in vitro when membranes derived from murine myeloma MOPC-46B cells were incubated in the presence of detergent, Mg^{2+}, and Mn^{2+} at pH 7.4 (44, 45). Later, OSPs were seen when calf thyroid microsomes were incubated with radiolabeled $Glc_{3\text{-}0}Man_9GlcNAc_2$-PP-dolichol in the presence of detergent and Mn^{2+} at pH 7.0 (26). Further in vitro studies with yeast microsomes indicated OSP generation from $Man_{8\text{-}9}GlcNAc_2$-PP-dolichol in the presence of detergent at pH 7.5 (14). This yeast activity is increased by 50% in the presence of 10 mM Ca^{2+} or Mn^{2+} ions and reduced by 50% in the presence of EDTA (14). More recently, cation-dependent OSP generation (Mn^{2+} >> Mg^{2+} and Ca^{2+}) was observed when microsomes were incubated with radiolabeled $Man_5GlcNAc_2$-PP-dolichol in the presence of detergent at pH 7.4 (12). However, none of these studies addressed the potential selectivity of the reaction for DLO, and although the activities are described as pyrophosphatases (diphosphatases) because OSPP were not detected, formal demonstration of a DLO diphosphatase was not attempted. In order to characterize this activity more fully, we reexamined its ion dependence and found that although OSPs are released from DLO in the presence of Mn^{2+} at pH 7.5, Co^{2+} activation of OSP release is more efficient at this pH. Then, fine-tuning of the assay revealed a striking increase in Co^{2+}-provoked OSP release at lower pH values. At these lower pH values, Mn^{2+} possessed little ability to activate OSP release, and data shown in Fig. 4A demonstrate that at pH 5.5 Mn^{2+} inhibits Co^{2+}-activated OSP release and that increasing the Co^{2+} concentration can relieve this inhibition. These data suggest that the previously described mammalian Mn^{2+}-dependent OSP-generating activity is the same as the activity we have characterized. In view of the very low levels of cobalt in cells, the physiological relevance of the ion dependency of the DLODP activity remains to be ascertained.

Are the biochemical characteristics of DLODP similar to other lipid phosphatases?

The biochemical characteristics of the DLODP activity described here are quite different from those of the previously described DolP and DolPP phosphatase activities. In mammalian cells, Dolpp1 [Saccharomyces *cerevisiae*: Cax4p/Cwh8p (52)] is a cation-independent, mainly DolPP- and, to a lesser extent, DolP-hydrolyzing, enzyme (53). The yeast

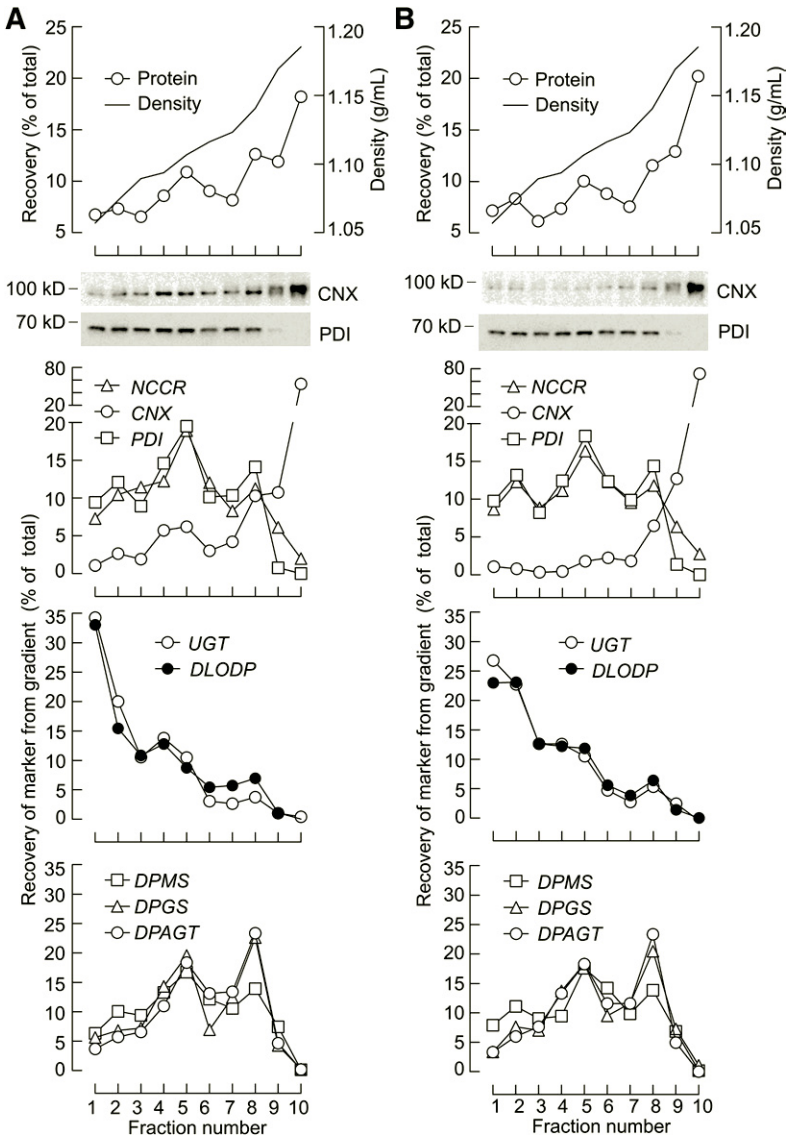

Fig. 8. Density gradient centrifugation of mouse liver microsomal membranes. Mouse liver microsomal pellets (P4) derived from homogenates generated using either a Potter-Elvehjeim (A) or Dounce (B) apparatus were fractionated on OptiPrep density gradients as described in Materials and Methods. The fractionation was monitored by measuring the density of the fractions and quantitating protein (upper panels). ER membranes were identified by measuring *NCCR* activity, and quantitating calnexin and PDI after SDS-PAGE and Western blotting (second panels). Membranes of the GA were identified by assaying *UGT*, and DLODP activity was measured using the standard assay. In the lower panels, data from DPMS, DPGS, and DPAGT assays are shown. For all panels, total activities or densitometric units (derived from scans of the Western blots) recovered from the gradient were computed, and the percentages of these totals recovered in each fraction are shown. The data in each panel are derived from a single experiment.

cwh8Δ strain manifests glycoprotein hypoglycosylation (52) consistent with the involvement of Cwh8p in recycling of DolPP (53, 54). In *S. cerevisiae,* DolPP is hydrolyzed by the cation-independent LPP1 (55, 56) and DPP1 (55, 57), lipid phosphate phospohydrolase 1 and diacylglycerol pyrophosphate phosphatase 1, respectively. Mammalian LPP-type enzymes (*Homo sapiens*: LPP1/PPAP2A, LPP2/PPAP2C, LPP3/PPAP2B) have broad substrate specificities and are capable of hydrolyzing PA and DGPP, as well as a range of other substrates including sphingosine 1-phosphate, ceramide 1-phosphate, and LPA (58). Certain mammalian DPP-type enzymes (PDP1/PPAPDC) also cleave farnesyl-PP and geranylgeranyl-PP (59). The function, if any, of these proteins in the regulation of the dolichol cycle remains unclear as in *S. cerevisiae* the *dpp1Δlpp1Δ* strain shows no hypoglycosylation phenotype. The cation dependence of the DLODP activity seems to rule out the possibility that one of the above-described cation-independent gene products could account for its activity. Although there are cation-dependent, N-ethylmaleimide-sensitive PA phosphatases (*S. cerevisiae*: PAH1; *H. sapiens*: LIPIN1, LIPIN2, and LIPIN3), these enzymes are unlikely candidates for DLODP activity because they are activated predominantly by Mg^{2+} and appear to have strict specificity for PA (60).

What is the physiological substrate of DLODP?

When various compounds were added to the DLODP assay mixture, it was found that many physiologically occurring water-soluble mono-, di-, and triphospho compounds inhibited the reaction at relatively high concentrations, whereas more lipophilic structures such as isoprenoid diphosphates, PA, and LPA inhibited the reaction more effectively. It should be pointed out that although LPA displayed a relatively low IC_{50}, maximum DLODP assay inhibition was not achieved at even 100 μM, thus making LPA an unlikely substrate for DLODP in vivo. $GlcNAc_2$-PP-solanesol is a substrate for DLODP and was found to inhibit the release of [^{3}H]OSP from [^{3}H]DLO about 10-fold more effectively than solanesyl-PP, indicating that DLODP interacts selectively with lipophilic diphosphodiesters such as DLO. To summarize, although our results point to a novel enzyme selective for DLO hydrolysis, it

remains a possibility that the DLODP activity that is described here is due to a previously characterized enzyme whose capacity to hydrolyze DLO has yet to be reported. Whatever the true physiological substrate of this DLODP activity, our selectivity studies reinforce the hypothesis that it hydrolyzes DLO in vivo.

What is the relationship between DLODP and cellular OSP-generating mechanisms?

Our subcellular fractionation data demonstrate that the bulk of DLODP activity does not codistribute with markers of the ER but fractionates in lighter membranes similar to those containing GA-situated UGT. The GA has previously been shown to harbor a cation-independent DolPP phosphatase activity that is inhibited by Mn^2, but the identity of this enzyme has not been established at the molecular level (61). The definitive subcellular localization of the DLODP activity will depend on the availability of an antibody to the protein. Nevertheless, although our subcellular fractionation data cannot rule out the possibility that small amounts of DLODP activity are associated with ER membranes, they clearly demonstrate that the majority of DLODP activity does not codistribute with markers of either the smooth or rough ER or key enzymes involved in DLO biosynthesis. Our results are in agreement with classical subcellular fractionation studies in liver homogenates in which enzymes of the dolichol cycle such as DPAGT, DPGS and DPMS were demonstrated to cofractionate with markers of the ER (62). DLO itself is also associated with heavy microsomal membranes associated with the ER. The behavior of DLODP during subcellular fractionation suggests that either the bulk of this activity is not involved in DLO regulation or DLO regulation by this enzyme occurs in regions of the cell where DLO biosynthesis and OST-mediated protein *N*-glycosylation do not occur. What is the evidence that OSP generation is associated with the ER? The question of the localization of OSP generation in living cells has not been addressed. Our previously reported data showed that liberation of OSP from truncated DLO intermediates occurs efficiently in streptolysin O-permeabilized Epstein-Barr virus-transformed lymphoblasts incubated in the absence of ATP and cytosol (11), conditions where vesicular transport is blocked. Furthermore, OSP production was reduced when incubations were carried out in the presence of an *N*-glycosylation acceptor peptide. The ensemble of these data indicates that OSP generation from truncated DLO occurs in a compartment that is functionally contiguous with the ER. Although, as mentioned above, vesicular ER-to-Golgi transport of protein and lipid requires cytosolic factors and ATP, it is known that when using either semi-intact cell systems or broken cell preparations to assay nonvesicular lipid transport mechanisms (63), even ATP-dependent processes may lose their ATP dependence when assays are carried out at 37°C (64). Potentially, therefore truncated DLO could be transported to a post-ER compartment by a nonvesicular, ATP-independent, or even ATP-dependent process in streptolysin O-permeabilized cells. To summarize, the precise site or sites of OSP generation in living cells is not known. Our results demonstrate that the bulk of DLODP activity associates with membranes that are lighter than those containing other enzymes of the dolichol cycle. The origin of these membranes, whether from a subdomain of the ER or a post-ER compartment such as the GA remains to be determined. Finally, the distinct subcellular localizations of the catabolic DLODP-mediated reaction, on the one hand, and the biosynthetic reactions of the dolichol cycle, on the other, may have arisen to allow DLO control in the absence of unwanted destruction of useful DLO.

What are the potential functions of DLODP?

Previous studies have shown that in liver the GA contains more dolichol/dolichol fatty acyl esters than either the smooth or rough ER. Conversely, the ER is richer in DolP than the GA (65, 66). Based on these facts, and other studies indicating that the GA is enriched in DolPP diphosphatase activity and dolichol kinase activity is found in the ER (61), it has been proposed that should DolPP escape the ER into the GA, it is rapidly transformed into dolichol or DolP and then returned to the ER (61). A post-ER DLODP activity could perform the same function on truncated "unchaperoned" DLO intermediates that escape the ER-situated DLO biosynthetic machinery and flow out of the ER. The function of this activity may not be DolP recycling per se, but rather the elimination of potentially toxic DLO that escapes the ER.

The authors thank Professor Sonia Karabina for critical reading of the manuscript.

REFERENCES

1. Haltiwanger, R. S., and J. B. Lowe. 2004. Role of glycosylation in development. *Annu. Rev. Biochem.* **73:** 491–537.
2. Jaeken, J. 2011. Congenital disorders of glycosylation (CDG): it's (nearly) all in it! *J. Inherit. Metab. Dis.* **34:** 853–858.
3. Aebi, M., and T. Hennet. 2001. Congenital disorders of glycosylation: genetic model systems lead the way. *Trends Cell Biol.* **11:** 136–141.
4. Frank, C. G., S. Sanyal, J. S. Rush, C. J. Waechter, and A. K. Menon. 2008. Does Rft1 flip an N-glycan lipid precursor? *Nature.* **454:** E3–E5.
5. Rosenwald, A. G., J. Stoll, and S. S. Krag. 1990. Regulation of glycosylation. Three enzymes compete for a common pool of dolichyl phosphate in vivo. *J. Biol. Chem.* **265:** 14544–14553.
6. Kean, E. L., J. S. Rush, and C. J. Waechter. 1994. Activation of GlcNAc-P-P-dolichol synthesis by mannosylphosphoryldolichol is stereospecific and requires a saturated alpha-isoprene unit. *Biochemistry.* **33:** 10508–10512.
7. Spiro, M. J., and R. G. Spiro. 1991. Potential regulation of N-glycosylation precursor through oligosaccharide-lipid hydrolase action and glucosyltransferase-glucosidase shuttle. *J. Biol. Chem.* **266:** 5311–5317.
8. Harada, Y., R. Buser, E. M. Ngwa, H. Hirayama, M. Aebi, and T. Suzuki. 2013. Eukaryotic oligosaccharyltransferase generates free oligosaccharides during N-glycosylation. *J. Biol. Chem.* **288:** 32673–32684.
9. Cacan, R., C. Villers, M. Belard, A. Kaiden, S. S. Krag, and A. Verbert. 1992. Different fates of the oligosaccharide moieties of lipid intermediates. *Glycobiology.* **2:** 127–136.
10. Cacan, R., S. Duvet, D. Kmiecik, O. Labiau, A. M. Mir, and A. Verbert. 1998. 'Glyco-deglyco' processes during the synthesis of N-glycoproteins. *Biochimie.* **80:** 59–68.
11. Peric, D., C. Durrant-Arico, C. Delenda, T. Dupre, P. De Lonlay, H. O. de Baulny, C. Pelatan, B. Bader-Meunier, O. Danos, I. Chantret,

et al. 2010. The compartmentalisation of phosphorylated free oligosaccharides in cells from a CDG Ig patient reveals a novel ER-to-cytosol translocation process. *PLoS One.* **5:** e11675.
12. Vleugels, W., S. Duvet, R. Peanne, A. M. Mir, R. Cacan, J. C. Michalski, G. Matthijs, and F. Foulquier. 2011. Identification of phosphorylated oligosaccharides in cells of patients with a congenital disorders of glycosylation (CDG-I). *Biochimie.* **93:** 823–833.
13. Harada, Y., K. Nakajima, Y. Masahara-Negishi, H. H. Freeze, T. Angata, N. Taniguchi, and T. Suzuki. 2013. Metabolically programmed quality control system for dolichol-linked oligosaccharides. *Proc. Natl. Acad. Sci. USA.* **110:** 19366–19371.
14. Belard, M., R. Cacan, and A. Verbert. 1988. Characterization of an oligosaccharide-pyrophosphodolichol pyrophosphatase activity in yeast. *Biochem. J.* **255:** 235–242.
15. Dwivedi, R., H. Nothaft, B. Reiz, R. M. Whittal, and C. M. Szymanski. 2013. Generation of free oligosaccharides from bacterial protein N-linked glycosylation systems. *Biopolymers.* **99:** 772–783.
16. Bernardes, G. J., R. Kikkeri, M. Maglinao, P. Laurino, M. Collot, S. Y. Hong, B. Lepenies, and P. H. Seeberger. 2010. Design, synthesis and biological evaluation of carbohydrate-functionalized cyclodextrins and liposomes for hepatocyte-specific targeting. *Org. Biomol. Chem.* **8:** 4987–4996.
17. Busca, P., and O. R. Martin. 2004. Synthesis of UDP-GalNAc analogues as probes for the study of polypeptide-alpha-GalNAc-transferases. Part 2. *Tetrahedron Lett.* **45:** 4433–4436.
18. Fang, X., B. S. Gibbs, and J. K. Coward. 1995. Synthesis and evaluation of synthetic analogues of dolichyl-P-P-chitobiose as oligosaccharyltransferase substrates. *Bioorg. Med. Chem. Lett.* **5:** 2701–2706.
19. Mathiselvam, M., A. Srivastava, B. Varghese, S. Perez, and D. Loganathan. 2013. Synthesis and X-ray crystallographic investigation of N-(beta-D-glycosyl)butanamides derived from GlcNAc and chitobiose as analogs of the conserved chitobiosylasparagine linkage of N-glycoproteins. *Carbohydr. Res.* **380:** 37–44.
20. Scholte, A. A., and J. C. Vederas. 2006. Incorporation of deuterium-labelled analogs of isopentenyl diphosphate for the elucidation of the stereochemistry of rubber biosynthesis. *Org. Biomol. Chem.* **4:** 730–742.
21. Shpirt, A. M., L. O. Kononov, S. D. Maltsev, and V. N. Shibaev. 2011. Chemical synthesis of polyprenyl sialyl phosphate, a probable biosynthetic intermediate of bacterial polysialic acid. *Carbohydr. Res.* **346:** 2849–2854.
22. Tai, V. W., and B. Imperiali. 2001. Substrate specificity of the glycosyl donor for oligosaccharyl transferase. *J. Org. Chem.* **66:** 6217–6228.
23. Zamyatina, A., S. Gronow, M. Puchberger, A. Graziani, A. Hofinger, and P. Kosma. 2003. Efficient chemical synthesis of both anomers of ADP L-glycero- and D-glycero-D-manno-heptopyranose. *Carbohydr. Res.* **338:** 2571–2589.
24. Chapman, A., I. S. Trowbridge, R. Hyman, and S. Kornfeld. 1979. Structure of the lipid-linked oligosaccharides that accumulate in class E Thy-1-negative mutant lymphomas. *Cell.* **17:** 509–515.
25. Spiro, M. J., R. G. Spiro, and V. D. Bhoyroo. 1976. Lipid-saccharide intermediates in glycoprotein biosynthesis. I. Formation of an oligosaccharide-lipid by thyroid slices and evaluation of its role in protein glycosylation. *J. Biol. Chem.* **251:** 6400–6408.
26. Anumula, K. R., and R. G. Spiro. 1983. Release of glucose-containing polymannose oligosaccharides during glycoprotein biosynthesis. Studies with thyroid microsomal enzymes and slices. *J. Biol. Chem.* **258:** 15274–15282.
27. Moore, S. E., and R. G. Spiro. 1994. Intracellular compartmentalization and degradation of free polymannose oligosaccharides released during glycoprotein biosynthesis. *J. Biol. Chem.* **269:** 12715–12721.
28. Fleischer, S., and M. Kervina. 1974. Subcellular fractionation of rat liver. *Methods Enzymol.* **31:** 6–41.
29. Plonne, D., I. Cartwright, W. Linss, R. Dargel, J. M. Graham, and J. A. Higgins. 1999. Separation of the intracellular secretory compartment of rat liver and isolated rat hepatocytes in a single step using self-generating gradients of iodixanol. *Anal. Biochem.* **276:** 88–96.
30. Smith, P. K., R. I. Krohn, G. T. Hermanson, A. K. Mallia, F. H. Gartner, M. D. Provenzano, E. K. Fujimoto, N. M. Goeke, B. J. Olson, and D. C. Klenk. 1985. Measurement of protein using bicinchoninic acid. *Anal. Biochem.* **150:** 76–85.
31. Meister, A. 1950. Reduction of alpha gamma-diketo and alpha-keto acids catalyzed by muscle preparations and by crystalline lactic dehydrogenase. *J. Biol. Chem.* **184:** 117–129.
32. Srere, P. A., and Y. Matsuoka. 1972. Inhibition of rat citrate synthase by acetoacetyl CoA and NADH. *Biochem. Med.* **6:** 262–266.
33. Razzell, W. E. 1961. Tissue and intracellular distribution of two phosphodiesterases. *J. Biol. Chem.* **236:** 3028–3030.
34. Andersch, M. A., and A. J. Szczypinski. 1947. Use of p-nitrophenylphosphate as the substrate in determination of serum acid phosphatase. *Am. J. Clin. Pathol.* **17:** 571–574.
35. Wagner, R. R., and M. A. Cynkin. 1971. Glycoprotein metabolism: a UDP-galactose-glycoprotein galactosyltransferase of rat serum. *Biochem. Biophys. Res. Commun.* **45:** 57–62.
36. Richards, J. B., and F. W. Hemming. 1972. The transfer of mannose from guanosine diphosphate mannose to dolichol phosphate and protein by pig liver endoplasmic reticulum. *Biochem. J.* **130:** 77–93.
37. Chantret, I., J. Dancourt, T. Dupre, C. Delenda, S. Bucher, S. Vuillaumier-Barrot, H. Ogier de Baulny, C. Peletan, O. Danos, N. Seta, et al. 2003. A deficiency in dolichyl-P-glucose:Glc1Man9GlcNAc2-PP-dolichyl alpha3-glucosyltransferase defines a new subtype of congenital disorders of glycosylation. *J. Biol. Chem.* **278:** 9962–9971.
38. Williams, C. H., Jr., and H. Kamin. 1962. Microsomal triphosphopyridine nucleotide-cytochrome c reductase of liver. *J. Biol. Chem.* **237:** 587–595.
39. Lehrman, M. A., X. Y. Zhu, and S. Khounlo. 1988. Amplification and molecular cloning of the hamster tunicamycin-sensitive N-acetylglucosamine-1-phosphate transferase gene. The hamster and yeast enzymes share a common peptide sequence. *J. Biol. Chem.* **263:** 19796–19803.
40. Varki, A., and S. Kornfeld. 1983. The spectrum of anionic oligosaccharides released by endo-beta-N-acetylglucosaminidase H from glycoproteins. Structural studies and interactions with the phosphomannosyl receptor. *J. Biol. Chem.* **258:** 2808–2818.
41. Spiro, M. J., R. G. Spiro, and V. D. Bhoyroo. 1979. Glycosylation of proteins by oligosaccharide-lipids. Studies on a thyroid enzyme involved in oligosaccharide transfer and the role of glucose in this reaction. *J. Biol. Chem.* **254:** 7668–7674.
42. Kelleher, D. J., D. Karaoglu, and R. Gilmore. 2001. Large-scale isolation of dolichol-linked oligosaccharides with homogeneous oligosaccharide structures: determination of steady-state dolichol-linked oligosaccharide compositions. *Glycobiology.* **11:** 321–333.
43. Chantret, I., J. Dancourt, A. Barbat, and S. E. Moore. 2005. Two proteins homologous to the N- and C-terminal domains of the bacterial glycosyltransferase Murg are required for the second step of dolichyl-linked oligosaccharide synthesis in *Saccharomyces cerevisiae*. *J. Biol. Chem.* **280:** 9236–9242.
44. Baynes, J. W., A. F. Hsu, and E. C. Heath. 1973. The role of mannosyl-phosphoryl-dihydropolyisoprenol in the synthesis of mammalian glycoproteins. *J. Biol. Chem.* **248:** 5693–5704.
45. Hsu, A. F., J. W. Baynes, and E. C. Heath. 1974. The role of a dolichol-oligosaccharide as an intermediate in glycoprotein biosynthesis. *Proc. Natl. Acad. Sci. USA.* **71:** 2391–2395.
46. Adair, W. L., Jr., and N. Cafmeyer. 1989. Characterization of dolichyl diphosphate phosphatase from rat liver. *Chem. Phys. Lipids.* **51:** 279–284.
47. Scher, M. G., and C. J. Waechter. 1984. Brain dolichyl pyrophosphate phosphatase. Solubilization, characterization, and differentiation from dolichyl monophosphate phosphatase activity. *J. Biol. Chem.* **259:** 14580–14585.
48. Belocopitow, E., and D. Boscoboinik. 1982. Dolichyl-phosphate phosphatase and dolichyl-diphosphate phosphatase in rat-liver microsomes. *Eur. J. Biochem.* **125:** 167–173.
49. Rip, J. W., C. A. Rupar, N. Chaudhary, and K. K. Carroll. 1981. Localization of a dolichyl phosphate phosphatase in plasma membranes of rat liver. *J. Biol. Chem.* **256:** 1929–1934.
50. Strous, G. J., P. van Kerkhof, G. van Meer, S. Rijnboutt, and W. Stoorvogel. 1993. Differential effects of brefeldin A on transport of secretory and lysosomal proteins. *J. Biol. Chem.* **268:** 2341–2347.
51. Bergeron, J. J., M. B. Brenner, D. Y. Thomas, and D. B. Williams. 1994. Calnexin: a membrane-bound chaperone of the endoplasmic reticulum. *Trends Biochem. Sci.* **19:** 124–128.
52. van Berkel, M. A., M. Rieger, S. te Heesen, A. F. Ram, H. van den Ende, M. Aebi, and F. M. Klis. 1999. The *Saccharomyces cerevisiae* CWH8 gene is required for full levels of dolichol-linked oligosaccharides in the endoplasmic reticulum and for efficient N-glycosylation. *Glycobiology.* **9:** 243–253.
53. Rush, J. S., S. K. Cho, S. Jiang, S. L. Hofmann, and C. J. Waechter. 2002. Identification and characterization of a cDNA encoding a dolichyl pyrophosphate phosphatase located in the endoplasmic reticulum of mammalian cells. *J. Biol. Chem.* **277:** 45226–45234.

54. Fernandez, F., J. S. Rush, D. A. Toke, G. S. Han, J. E. Quinn, G. M. Carman, J. Y. Choi, D. R. Voelker, M. Aebi, and C. J. Waechter. 2001. The CWH8 gene encodes a dolichyl pyrophosphate phosphatase with a luminally oriented active site in the endoplasmic reticulum of *Saccharomyces cerevisiae*. *J. Biol. Chem.* **276:** 41455–41464.
55. Faulkner, A., X. Chen, J. Rush, B. Horazdovsky, C. J. Waechter, G. M. Carman, and P. C. Sternweis. 1999. The LPP1 and DPP1 gene products account for most of the isoprenoid phosphate phosphatase activities in *Saccharomyces cerevisiae*. *J. Biol. Chem.* **274:** 14831–14837.
56. Furneisen, J. M., and G. M. Carman. 2000. Enzymological properties of the LPP1-encoded lipid phosphatase from *Saccharomyces cerevisiae*. *Biochim. Biophys. Acta.* **1484:** 71–82.
57. Wu, W. I., Y. Liu, B. Riedel, J. B. Wissing, A. S. Fischl, and G. M. Carman. 1996. Purification and characterization of diacylglycerol pyrophosphate phosphatase from *Saccharomyces cerevisiae*. *J. Biol. Chem.* **271:** 1868–1876.
58. Carman, G. M., and G. S. Han. 2006. Roles of phosphatidate phosphatase enzymes in lipid metabolism. *Trends Biochem. Sci.* **31:** 694–699.
59. Miriyala, S., T. Subramanian, M. Panchatcharam, H. Ren, M. I. McDermott, M. Sunkara, T. Drennan, S. S. Smyth, H. P. Spielmann, and A. J. Morris. 2010. Functional characterization of the atypical integral membrane lipid phosphatase PDP1/PPAPDC2 identifies a pathway for interconversion of isoprenols and isoprenoid phosphates in mammalian cells. *J. Biol. Chem.* **285:** 13918–13929.
60. Harris, T. E., and B. N. Finck. 2011. Dual function lipin proteins and glycerolipid metabolism. *Trends Endocrinol. Metab.* **22:** 226–233.
61. Wolf, M. J., J. S. Rush, and C. J. Waechter. 1991. Golgi-enriched membrane fractions from rat brain and liver contain long-chain polyisoprenyl pyrophosphate phosphatase activity. *Glycobiology.* **1:** 405–410.
62. Ravoet, A. M., A. Amar-Costesec, D. Godelaine, and H. Beaufay. 1981. Quantitative assay and subcellular distribution of enzymes acting on dolichyl phosphate in rat liver. *J. Cell Biol.* **91:** 679–688.
63. Lev, S. 2010. Non-vesicular lipid transport by lipid-transfer proteins and beyond. *Nat. Rev. Mol. Cell Biol.* **11:** 739–750.
64. Kumagai, K., M. Nishijima, and K. Hanada. 2012. Reconstitution assay system for ceramide transport with semi-intact cells. *Methods Cell Biol.* **108:** 117–129.
65. Rip, J. W., N. Chaudhary, and K. K. Carroll. 1983. Distribution and metabolism of dolichol and dolichyl phosphate in rat liver. *Can. J. Biochem. Cell Biol.* **61:** 1025–1031.
66. Rip, J. W., N. Chaudhary, and K. K. Carroll. 1983. The submicrosomal distribution of dolichyl phosphate and dolichyl phosphate phosphatase in rat liver. *J. Biol. Chem.* **258:** 14926–14930.
67. Huyer, G., S. Liu, J. Kelly, J. Moffat, P. Payette, B. Kennedy, G. Tsaprailis, M. J. Gresser, and C. Ramachandran. 1997. Mechanism of inhibition of protein-tyrosine phosphatases by vanadate and pervanadate. *J. Biol. Chem.* **272:** 843–851.